



ELSEVIER

Earth and Planetary Science Letters 193 (2001) 631–642

EPSL

www.elsevier.com/locate/epsl

Detection of low concentrations of fine-grained iron oxides by voltammetry of microparticles

I.H.M. van Oorschot^{a,*}, T. Grygar^b, M.J. Dekkers^{a,c}

^a *Utrecht University, Paleomagnetic laboratory 'Fort Hoofddijk', Budapestlaan 17, 3584 CD Utrecht, The Netherlands*

^b *Institute of Inorganic Chemistry, Academy of Sciences of the Czech Republic, 250 68 Řež, Czech Republic*

^c *CEREGE, P.O. Box 80, 13545 Aix en Provence Cedex 4, France*

Received 17 May 2001; received in revised form 17 August 2001; accepted 5 September 2001

Abstract

Mineralogical discrimination of iron oxides in soils and sediments is not a trivial task, mainly because of their small grain size and low concentration. With mineral–magnetic techniques, highly magnetic ferrimagnetic spinels can be determined with a very low detection limit (~ 10 ppm). Unfortunately, the magnetic signal of natural samples is often dominated by magnetite, and in particular the expression of weakly magnetic antiferromagnetic minerals is suppressed by this high signal. In contrast, electrochemical techniques, such as voltammetry of microparticles (VMP) are not affected by these differences in magnetic signal. VMP makes use of the electrochemical law that iron(oxy)(hydr)oxides can be reductively dissolved at potentials that are specific for their mineralogy and reactivity. Therefore, by scanning over a potential range and monitoring the potential at which a reaction occurs, one can specify the type of minerals present. VMP can be applied to samples without requiring any form of pre-treatment. The method is rapid, comparatively straightforward to interpret, and requires little amount of sample (μg). However, the detection limit of VMP on natural samples has not yet been investigated. Here, we present a pilot study of the use of VMP in the identification of the ferric oxides of natural samples from Spanish red beds of Miocene age. A standard addition method with pyrolusite as internal standard enabled semi-quantitative analysis of the samples; concentrations of (anti)ferromagnetic iron(oxy)(hydr)oxides down to ~ 0.1 wt% could be detected. © 2001 Elsevier Science B.V. All rights reserved.

Keywords: electrochemical properties; soil surveys; magnetite; hematite; goethite; magnetic minerals

1. Introduction

Qualitative and quantitative identification of magnetic minerals is essential to a successful understanding of mineral–magnetic climate pro-

xies. The presence of strongly magnetic ferrimagnetic minerals in a sample – the rule in natural samples – suppresses the expression of the weakly magnetic antiferromagnetic minerals. By careful application of a number of different rock-magnetic techniques (i.e. first-order reversal curve (FORC) analysis, isothermal remanent magnetisation (IRM) component analysis, thermomagnetic analysis, and determination of the frequency dependence of susceptibility), the magnetic mineral-

* Corresponding author. Tel.: +31-30-253-1361;

Fax: +31-30-253-1677.

E-mail address: oorschot@geo.uu.nl (I.H.M. van Oorschot).

ogy of a sample can be derived. However, this is a fairly time-consuming procedure, and it unfortunately does not always yield unambiguous results. More generally applied mineralogical identification methods such as X-ray diffraction and Moessbauer spectroscopy, are often not suited for use on natural material, because the magnetic components are of low concentration and usually fall below the detection limit of these techniques. Conversely, selective extraction techniques have yielded promising results for the identification of the magnetic carriers in natural samples [1–3]. However, these methods still require additional mineral–magnetic techniques for a complete understanding of the sample composition. To avoid possible ambiguity in the interpretation, as well as laborious analytical procedures, a mineral-specific analytical technique is needed, which can identify different types of magnetic minerals, even at low concentrations.

1.1. *Voltammetry of microparticles (VMP)*

Electrochemistry describes the use of chemical reactions to produce electricity, and the use of electricity to produce a chemical change [4]. Thus, it can be used to study the mechanism and kinetics of redox reactions. For a long time, it was generally accepted that only species in solution could be studied with electroanalytical techniques. However, in 1989, Scholz and co-workers [5] introduced a method of sufficient reproducibility and lucidity, where the solid sample was immobilised on the electrode surface and subsequently analysed. This method was named abrasive stripping voltammetry (AbrSV), later the name was changed to VMP.

With VMP, information on the electroactive compounds in the sample is obtained by scanning over a specified potential range and looking for peaks in the current, which indicate the occurrence of electrochemical reactions. The current peaks and starts to decrease when a significant amount of the reacting species is consumed. The plot of the potential vs the current is called a voltammogram or VA curve. The peak potential is indicative of the compounds that have reacted, and the peak area (or charge) is proportional to

the amount of the electroactive species [6]. In this way, information on the concentration and chemical state of the solid reactants, as well as on the reaction kinetics and mechanism can be obtained [7]. Voltammetry is complementary to standard techniques for identification of powdered solids (e.g. X-ray diffraction, IR-spectroscopy, Moessbauer spectroscopy), but it is also rapid, simple, and works on a microscale. It is suitable for analysing metal alloys, pigments, superconductors, and pure minerals, but application to mixtures of inorganic compounds or even natural soil and rock samples is possible as well [7].

Grygar [8] studied the reductive dissolution behaviour of several synthetic iron oxides and oxyhydroxides (hematite, magnetite, maghemite and goethite) with VMP. He found that these minerals are reductively dissolved from the working electrode at different potentials typical of each phase, illustrating the diagnostic power of this technique. It is also possible to quantify concentrations of different minerals within a mixture, by making a calibration curve with mixtures of known amounts of well-defined minerals [8,9]. Comparison of the results of the electrochemical studies of reductive dissolution with normal reductive dissolution experiments has shown that there is a close similarity between the chemical and electrochemical dissolution of iron oxides, including the relative reactivity of individual iron oxides and the influence of the particle size. Electrochemical methods are therefore a valid alternative to more laborious and time-consuming methods of mineral identification through selective dissolution.

VMP could make it possible to derive the composition and characteristics of the ferric oxides in a sample within a matter of minutes. Furthermore, the technique is simple and no sample pre-treatment is required (apart from grinding in a pestle and mortar). In particular for weakly magnetic material such as hematite and goethite, VMP would complement standard mineral–magnetic techniques. However, the method has as yet only been tested on synthetic material and on some lateritic samples containing high concentrations of iron oxides [10–12]. Here, we present the results of a pilot study concerning the analysis of

the magnetic mineral composition in natural samples containing low concentrations of α -Fe₂O₃ and α -FeOOH with VMP.

2. Experimental procedures

2.1. Samples and magnetic methods

Samples were taken from a 25-m long transect of continental red bed deposits in La Gloria, Teruel basin, Spain (Fig. 1a). This section dates from the Middle to Late Miocene (~ 8.3 – ~ 11.4 Ma), and consists mainly of red silty clays with intercalation of red sands and conglomerates. It is capped by white lacustrine limestones [13] (Fig. 1b). During red bed deposition, the climate in the Teruel Basin was warm and semi-arid to arid [14]. The samples are labelled as GLOxxA, with xx the number of the sample starting with 01 at the bottom. The samples used in this study come from an interval close to the middle of the transect at ~ 10 -m stratigraphic level. This part of the section was formed in the Late Miocene (~ 9.8 Ma), and contains an alternation of red clay, red sands and sandy conglomerates. In Table 1, some geochemical, lithological and magnetic characteristics of the samples are presented.

The magnetic composition of the samples was analysed by IRM component analysis and FORC distribution analysis. The samples (1–2 g) for IRM component analysis were weighed into plastic cylindrical cups and mixed with epoxy resin (Araldit D, Hardener HY956, Ciba Specialty Chemicals). IRM was induced by a PM4 pulse magnetiser and measured with a JR5A spinner magnetometer (AGICO). The sensitivity of the spinner magnetometer is $\sim 2.7 \times 10^{-11}$ Am², the minimum IRM measured during our experiments was at least two times stronger. IRM acquisition curves (completely saturated) were analysed with the Cumulative Log Gaussian (CLG) programme of Kruiver et al. [15] and the automated analysis method by Heslop et al. [16] to determine magnetic coercivity components in the samples. This involves fitting of a measured IRM acquisition

curve with a number of logarithmically distributed coercivity distributions, each characterised by their midpoint ($B_{1/2}$), spreading or dispersion, and magnetic concentration. A statistical test is provided to determine the number of distributions required for an optimal fit.

For the FORC analysis, samples (~ 10 mg) were mixed with epoxy resin and cast in Teflon moulds, which resulted in cylindrical samples with a diameter of ~ 1.5 mm and a length of maximum ~ 2 mm. Data acquisition was performed on an alternating gradient magnetometer (MicroMag), and the results were plotted in a FORC diagram according to the methods described by Pike et al. [17–19]. A FORC distribution is a contour plot that allows the user to evaluate magnetic hardness and interaction separately in a sample. The horizontal axis ($\mu_0 H_c$) represents the coercivity, and the vertical axis ($\mu_0 H_u$) represents the magnetic interaction in the sample.

2.2. VMP procedure

The procedure for VMP is discussed in detail by Scholz and co-workers [5,7,20]. The following is a short description of the electrode and sample preparation, the voltammetric measurement, and the cleaning of the electrode. The specific settings for analysis of iron oxides were discussed by Grygar [10,12,21–23], and a brief summary of the settings is given in Fig. 2. Calculation of the concentration of measured compounds is done by using an internal standard as proposed by Grygar and van Oorschot [24], the details are discussed in Section 2.2.3.

The sensitivity of the VMP technique is essential for the purpose of application to natural samples. We tested the sensitivity by comparing untreated samples and samples that were extracted for a maximum of four times with the acid–ammonium–oxalate/ferrous–iron extraction method described by van Oorschot and Dekkers [25]. Previous mineral–magnetic studies have shown that this method preferentially attacks very fine-grained ferrimagnetic iron oxides, and thus enhances the magnetic signal of weakly magnetic antiferromagnetic hematite and goethite [3].

2.2.1. Preparation of the paraffin-impregnated graphite electrodes (PIGE) and electrochemical cell

To prevent contamination of the working electrode by material uptake from the electrolyte solution, PIGE are used [7]. A graphite rod of ~ 5 -cm length and ~ 5 -mm diameter is placed in a container with molten paraffin. Subsequently, the air is pumped out of the container to create a vacuum atmosphere, and thus facilitate the impregnation of the graphite by the molten paraffin. When air bubbles stop evolving from the electrode (after a few tens of minutes up to a few hours, depending on the original porosity of the graphite), it is fully impregnated. The electrode is taken out of the paraffin and cooled on filter paper. The lower end of the PIGE (which will be used to deposit the sample onto) is carefully polished on filter paper. The other end of the electrode is connected to a potentiostat with a crocodile clip.

The samples are ground to fine powder in an agate mortar to prevent preferential uptake of one compound by the electrode, this is especially important when a mixture of electroactive compounds is studied (the rule when dealing with natural samples) [7]. A small amount (mg) of the powdered sample is placed on a flat surface (preferably filter paper) and the electrode is rubbed over the sample. In this way, the sample particles are embedded into the soft surface of the graphite electrode. The total amount of sample that is in this way transferred onto the lower end of the electrode lies in the range of 0.1–2 μg [9]. By mixing an internal standard (with known mass and peak potential) into the sample before applying it to the working electrode, it is possible to quantitatively analyse the sample composition [24] (see also Section 2.2.3).

The PIGE is the working electrode on which the reactions take place. The electrochemical cell (Fig. 2) further consists of a platinum wire, which serves as counter electrode and provides electrons necessary for the reduction of iron. The reference electrode is a saturated calomel electrode (SCE), the supporting electrolyte is a N_2 -deaerated acetate buffer (acetic acid:acetate ratio 1:1, total acetate 0.2 M).

2.2.2. Measurement

The PIGE working electrode is dipped into the electrolyte solution and then slightly raised to make the solution adhere to the electrode surface. For reductive dissolution of the sample, a potentiostat ($\mu\text{Autolab}$, EcoChemie) is used to vary the potential of the system at a constant scan rate, from more positive to more negative and thus more reducing values, and the resulting current is measured. The potential range is limited to the chemical characteristics of the electrolyte. Since the electrolyte is usually an acid dissolved in water, the negative frame of the potential window is limited by the reduction of H^+ to H_2 at potentials beyond -1 V vs SCE. This reaction causes an exponential increase in the background current. In this study, the potential range was set between $+0.3$ and -1.2 V against SCE. Despite the rapid increase in background current over the -1 - to -1.2 -V interval, sometimes peaks could be discerned in this range. The scan rate in VMP is usually in the range of 1–50 mV/s. A high scan rate increases the peak current, but it also decreases the time in which a certain reaction can occur. This can cause distortion of the peaks to barely distinguishable kinks in the background current. On the other hand, a low scan rate will increase the background current, therefore it is best to empirically determine the optimum scan rate for each study. Here, the scan rate was set at 4 mV/s after optimisation in trial runs. Voltammograms of several subsamples from the same layer essentially yielded the same results.

Depending on the scan rate, the potential range, reaction kinetics, and particle size, a voltammetry measurement is usually very rapid and can be performed in 10 min or less [5]. The maximum measurement time in our experiments was ~ 6 min per scan. The samples all reacted fully in one scan, all consecutive scans were similar in shape and showed only the background current. To reduce the contribution of the background current, we scanned each sample twice and subtracted these two currents.

After the measurement, the electrode is cleaned by rubbing it on filter paper. Whether the cleaning was sufficient can be tested by measuring a voltammogram of the cleaned electrode, this should

give no peaks. From time to time it is recommendable to use a fine abrasive material for electrode cleaning. Here, we used SiO₂ powder (particle size ~10 µm) on a filter paper. The cleaned electrode can be used again to measure other samples. Because of the cleaning and polishing of the electrode surface, the PIGE will gradually decrease in size after each experiment. This has no significant effect on the measurement, and each electrode can be used numerous times. The same is valid for the electrolyte solution; because the ratio of solution to solid is very high, a large number of analyses can be performed before the electrolyte is saturated or interferes with the analysis.

2.2.3. Qualitative analysis and semi-quantitative analysis

2.2.3.1. Qualitative analysis To identify the ferric oxide species in the samples, we compared their peak potentials to those of synthetic samples of known composition. These samples were made from synthetic Fe oxides mixed into a quartz matrix with Fe oxide contents varying between 0.1 and 3 wt% (Table 2). Discrimination between goethite and hematite in the voltammograms is not straightforward, because of the overlap in the reaction potential range. Similar reactivity of both minerals can result in a similar reaction potential. By heating the samples for 15 min at 300°C, goethite is converted to poorly crystalline hematite. This causes a shift of the peak potential toward more positive values [21]. Comparison of the voltammograms of original and heated samples allows discrimination between these two minerals [24].

2.2.3.2. Semi-quantitative analysis

The amount of sample deposited on the working electrode cannot be exactly determined, this complicates the quantitative evaluation of voltammetric curves. Grygar and van Oorschot [24] explored standard addition as a quantification method and judged pyrolusite (β-MnO₂) to be the best internal standard for the (semi-)quantitative analysis of iron(oxy)(hydr)oxides. Mn(III,IV) oxides are reductively dissolved under similar conditions as Fe oxides [26] but at potentials by at least 0.5 V more positive (all potentials mentioned are valid for the experimental conditions as described in the previous sections, and are measured against SCE). The pyrolusite peak occurs at +0.30 V, therefore there is no interference with the peaks from our samples (Fig. 3a). However, VMP tests of the samples made with synthetic iron oxides and an internal standard, surprisingly showed that the peak heights of Mn- and Fe-oxide reductive dissolution were not in the proportion expected based on the oxide weight and the stoichiometry of the corresponding dissolution reaction. The areas of the Fe oxide peaks were 2–10 times larger than theoretically expected (Table 2). Magnetite, ferrihydrite, and Al-doped hematite were least increased, while the peaks of goethite and pure hematite were enhanced 7–10 times. Because these ‘enhancements’ were reproducible, we used these factors in the quantification of our natural samples. The tests further showed that the VMP detection limit for the synthetic samples with quartz matrix is ~0.1 wt% for hematite and goethite.

The voltammetric curves of all samples with the internal standard were processed with the GPES

Table 1
Some lithological, mineral–magnetic and geochemical parameters of the samples used in this study

Sample code	Stratigraphic level (cm)	Lithology	Colour	CaCO ₃ (wt%)	Fe (wt%)	Al (wt%)	k (10 ⁻⁶ SI)	B _{cr} /B _c	M _{rs} /M _s
GLO059A	900	dark red clay	5YR4/8	4.6	~3	~6	230	2.73	0.36
GLO062A	975	sandy red clay	5YR4/4	1.2	~1	~2.5	50	5.59	0.35
GLO065A	1080	limestone	5YR6/4	41.0	–	–	110	–	–
GLO066A	1120	caliche	5YR5/6	18.2	–	–	150	3.37	0.34

Colour is categorised with Munsell’s system for soil colour, iron and aluminium content of the samples is determined with total destruction (dissolution in a HF, HNO₃, and HClO₄ mixture). – No data acquired.

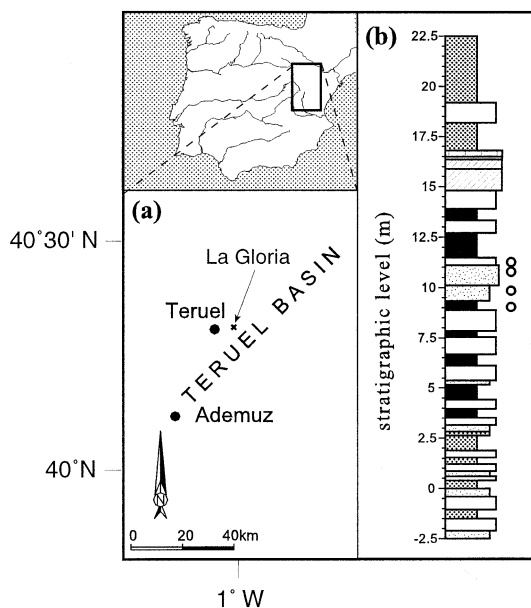


Fig. 1. (a) Topographical map of the location, the inset (b) shows the lithological column. The La Gloria section consists of a sequence of red clays (black and grey) intercalated with red sands (dotted) and limestones or caliches (white). The open circles adjacent to the lithological column, indicate the levels from which samples were taken for this study.

4.4 code as supplied by the manufacturer of the potentiostat (EcoChemie). This programme is suitable for the evaluation of currents of fully separated peaks. However, voltammetric peaks overlapped in the la Gloria samples, therefore a different approach was used for these samples. A model fit with kinetics of the general reaction order between 0.9 and 1.5 was used. The model was based on Butler–Volmer kinetics of the charge transfer, combined with a finite amount of reactive sites on the dissolving surface as well as a continuous distribution of the size and reactivity of the dissolving particles [12,22]. In this way individual peaks could be modelled (Fig. 3b) and from the changes in charges, the separate contributions of the peaks to the total signal could be calculated. Comparison of the I_{C1}/I_{C2} ratio between original and extracted samples gives an indication of the species that was dissolved by the AAO-Fe²⁺ extraction method (Fig. 3c).

3. Results

3.1. Magnetic measurements

The total SIRM values of these samples vary in the same way as their susceptibility, with high values for GLO59A and GLO66A and low values for GLO65A (Table 3). The behaviour of sample GLO62A is slightly different, with a minimum in susceptibility but not a minimum in SIRM. This suggests a different magnetic composition than the other samples, which was confirmed by the IRM component analysis. The magnetic composition of all samples is that of a two-component system with single domain (SD) to pseudo single domain (PSD) magnetite and hematite or goethite. The contribution of magnetite ($B_{1/2} \sim 25$ mT) is ~ 45 – 50% , while that of hematite ($B_{1/2} \sim 450$ mT) is 50 – 55% . Because of the differences in magnetisation between magnetite and hematite/goethite, the concentration of the former must therefore be much smaller than that of the latter minerals. GLO62A deviates in magnetic composition; it has a higher contribution of magnetite ($\sim 72\%$ of the total SIRM) as well as a

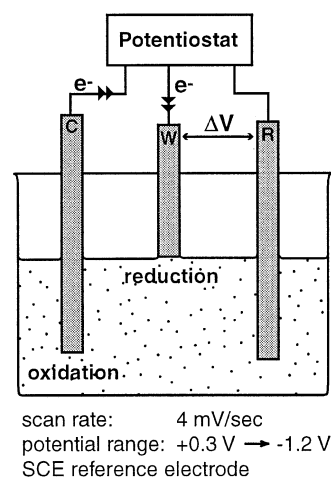


Fig. 2. Schematic representation of the electrochemical cell used in this study. C is the counter electrode (platinum wire), W is the working electrode (PIGE) and R the reference electrode (SCE). The potentiostat controls the potential of the working electrode and measures the current flowing through the electrode. The electrolyte is a deaerated mixture of acetic acid and acetate (1:1), with a total concentration of 0.2 M acetate.

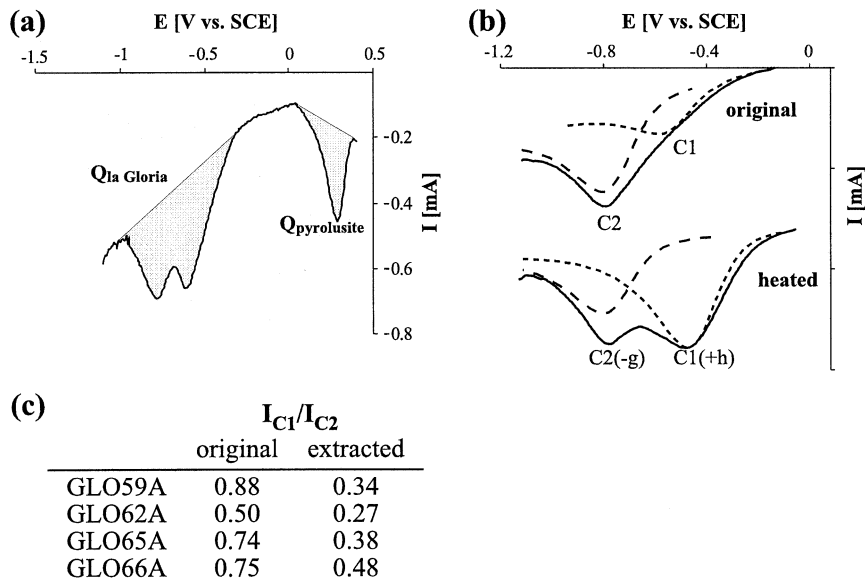


Fig. 3. Example of the calculation of the iron oxide concentrations, as well as the contribution of the different oxides to the C2 peak. (a) Shows a voltammogram of GLO62A, with pyrolusite added as an internal standard. The pyrolusite peak occurs at $\sim +0.3$ V (vs SCE). The charge of the pyrolusite peak can be related to its concentration. Subsequently, the charge of the other peaks is used to make an estimate of the concentration of iron oxides in the sample. (b) Shows an example of the calculation of the separate C1 and C2 signals from the total peak current of the overlapping two peaks. With Butler–Volmer fitting, the actual peaks are reconstructed (dotted line represents the C1 peak model curve, dashed line represents that of C2). The same is done for the voltammogram of the heated samples (15 min in air at 300°C). The changes in the individual peak currents are related to the conversion of goethite (g) to hematite (h) upon heating, and can be expressed as I_{C1}/I_{C2} . Comparison of this ratio for the original and the heated sample can be used to calculate the contribution of goethite to the C2 peak. Here, I_{C1}/I_{C2} of the original samples reflects the ratio of poorly crystalline hematite to well crystalline (hematite+goethite), and the same ratio for the heated samples represents the ratio of (poorly crystalline hematite+converted goethite) to well crystalline hematite. (c) Shows the difference in voltammogram of original and extracted samples as expressed by the current ratios. Here, the change in current ratio expresses the change in contribution of the poorly crystalline C1 hematite compared to the C2 species. The decrease of the ratio reflects the decrease in contribution of the C1 species after extraction.

higher average coercivity for both components ($B_{1/2}$ of ~ 56 and ~ 660 mT respectively).

After extraction with the AAO- Fe^{2+} method, three samples have lost part of both components and the contributions to the total signal have not changed greatly. However, in GLO62A, the dramatic change in relative contribution and $B_{1/2}$ of the soft component, indicates that here almost all fine-grained magnetite had been dissolved. For the other samples, the slight increase in $B_{1/2}$ of the soft component, suggests that part of the outer rims of the larger grains has been dissolved. Of the hard component, mostly poorly crystalline hematite was dissolved during extraction ($B_{1/2}$ increased slightly while its relative contribution remains approximately constant). However, in the

GLO62A samples, the contribution of the hard component increased considerably, while the $B_{1/2}$ decreased, this suggests the dissolution of goethite in these samples.

FORC diagrams are shown in Fig. 4. The presence of a soft magnetite component is evident as well as a much harder component. B_c of magnetite centres on ~ 16 mT in the FORC diagrams. Like in the IRM component analysis, the FORC diagram of GLO62A deviates from that of the other samples. The soft component shows a slightly lower B_c value, and there is a smoother transition toward the hard component. The magnetite could have a larger average grain size, it has a broader vertical spread in contours than the other GLO samples, indicating more interaction.

Table 2

Synthetic samples used to determine the specific reaction potentials of iron(hydr)oxides studied as well as for the semi-quantitative analysis

Sample code	Original Ep vs SCE (V)	Heated (300°C) Ep vs SCE (V)	Enhancement factor
Ferrihydrite	−0.33	−0.33 ^a	2
Magnetite	−0.26 (sh), −0.92	−0.28 (sh), −0.85	3
Goethite 1	−0.72	−0.44 ^a	6
Goethite 2	−0.69	−0.40 ^a	11
Goethite 3	−0.54	−0.35 ^a	8
Goethite 4	−0.73	−0.60 ^a	7
Hematite 1	−0.76	−0.75	10
Hematite 2	−0.72	−0.71	10
Hematite 3	−0.76	−0.76	3
Hematite 4	−0.83	−0.83	4

All samples were mixed with quartz, and concentration of iron(hydr)oxides varied between 0.1 and 3 wt%. The first column shows the peak potentials (EP) for the original samples, while the second column shows the peak potential after heating at 300°C for 15 min. The last column gives the relative enhancement of each signal compared to the signal expected from the peak height of the pyrolusite internal standard. All peak potentials were derived under the experimental conditions as described in the text.

There is more contour density closer to the left-hand side of the plot hinting at the presence of finer grains, possibly including SP grains.

3.2. Voltammetric measurements

The voltammetric curves of the samples from the La Gloria transect are clear, narrow and well reproducible. Voltammetry of the original samples exhibits two partly separated peaks C1 (~ -0.60 V) and C2 (~ -0.78 V) indicating the presence of at least two ferric oxide components

(Fig. 5A and Table 4). Sample GLO62A only exhibits the C2 peak. There are no indications of voltammetric kinks or shoulders at ~ -0.9 V in all samples, and therefore there is no voltammetric evidence for the presence of iron spinel oxides. The concentration lies below the detection limit of < 0.2 wt% for VMP.

The peak potential of C1 is indicative of poorly crystalline, soil ferric oxides. The C2 peak is comparable to peaks of well crystalline synthetic goethite or hematite (Table 2, adopted from [24]). The C1 peak disappears after AAO-Fe²⁺ extrac-

Table 3

IRM component analysis for the samples before and after extraction

Sample code	k (10^{-6} SI)	Total SIRM (10^{-3} Am ² /kg)	Component 1 (%)	$B_{1/2}$ 1 (mT)	Component 2 (%)	$B_{1/2}$ 2 (mT)
<i>Original samples</i>						
GLO059A	230	3.73	43.4	26.3 (11–63)	56.6	427 (151–1202)
GLO062A	50	1.75	72.2	56.5 (19–170)	27.8	659 (347–1259)
GLO065A	110	1.41	43.9	26.3 (10–69)	51.1	479 (209–1096)
GLO066A	150	2.28	48.9	25.7 (12–55)	56.1	437 (162–1175)
<i>Samples after AAO-Fe²⁺ extraction</i>						
GLO059A	135	2.89	42.9	91.2 (23–363)	57.1	417 (132–1318)
GLO062A	138	1.15	8.7	34.7 (15–81)	91.3	468 (166–1318)
GLO065A	112	1.16	40.5	32.4 (12–89)	59.5	525 (194–1413)
GLO066A	117	1.90	41.6	39.8 (15–110)	58.4	513 (170–1549)

Component 1 is the soft magnetic component, component 2 is the hard component. Besides the total SIRM of the samples and the relative contribution of each component, $B_{1/2}$ is given as the average $B_{1/2}$ value plus or minus one standard deviation (in brackets).

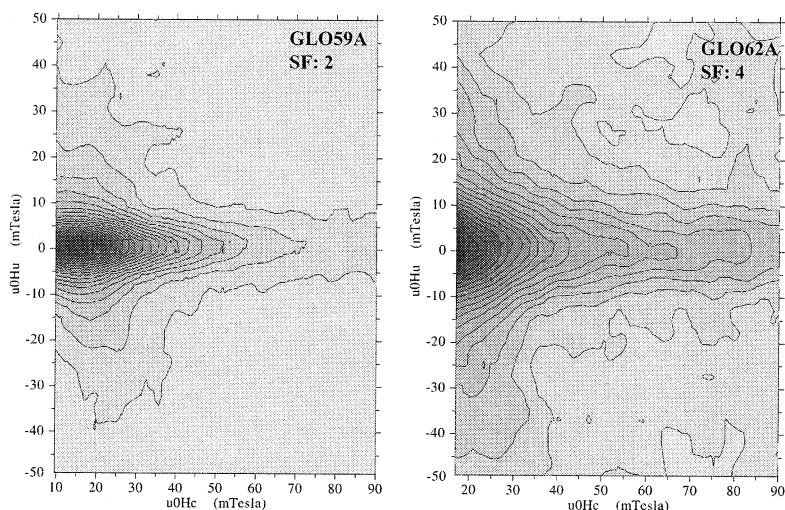


Fig. 4. FORC diagrams of La Gloria samples. The distribution along the horizontal axis is an indication for grain size (coercivity), while the distribution along the vertical axis represents magnetic interaction within the samples. The left panel is representative for all samples except GLO62A (right panel). The flat vertical distribution in the left panel indicates the presence of SD magnetite centred on $\mu_0 H_c$ of ~ 16 mT, while the wide distribution along the horizontal axis is caused by the presence of a hard magnetic component (hematite and/or goethite). In the right panel the signal is centred on lower field values, indicating the possible presence of SP grains. The vertical distribution is wider in the right panel, this can be caused by the presence of larger (PSD) magnetite grains or by a stronger signal from the hard magnetic component (hematite or goethite).

tion (Table 4, Fig. 5B), showing that the chemical reactivity of this ferric oxide fraction is bigger than that of the phases causing peak C2. After heating at 300°C, peak C1 only slightly shifts cathodically, therefore we attribute this peak to the reaction of poorly crystalline hematite. In contrast, the signal of C2 is redispersed to C1 and C2 after heating. This indicates that it is made up of a signal of several minerals, of which one converts hematite (C1 peak) upon heating. One of the minerals making up the signal of C2 has to be goethite, which is converted upon heating, thus decreasing the original C2 signal and increasing the C1 signal. Therefore, we attribute the C2 peak to a goethite–hematite assemblage, in which both phases have a practically equal dissolution reactivity. Because the extraction removed a substantial part of the poorly crystalline hematite, C1 disappears by extraction and reappears after heating due to the conversion of the remaining crystalline goethite to hematite. Here, as in the magnetic analysis, the behaviour of GLO62A deviates from that of the other samples. The C1 peak is absent in the original GLO62A sample, and it

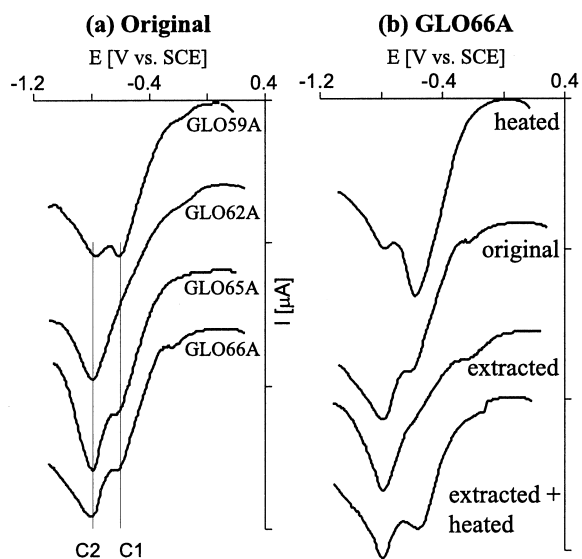


Fig. 5. (a) Voltammograms of the La Gloria samples. C1 and C2 denote the individual reductive dissolution peaks. (b) Voltammograms of sample GLO66A; original, heated for 15 min at 300°C, extracted by AAO- Fe^{2+} , and extracted and subsequently heated at 300°C. In both panels, the curves were offset for clarity.

Table 4

Peak potentials (V) detected in the VMP experiments for all samples (before and after extraction with AAO-Fe²⁺, as well as after heating to 300°C)

Sample code	Lithology	Original		Heated (300°C)		Extracted AAO-Fe ²⁺		Extracted and heated	
		C1	C2	C1	C2	C1	C2	C1	C2
GLO059A	dark red clay	-0.61	-0.76	-0.56	-0.82 (sh)	(sh)	-0.77	-0.6 (sh)	-0.81
GLO062A	sandy red clay	(sh)	-0.78	-0.49	-0.80	(np)	-0.77	-0.55 (sh)	-0.81
GLO065A	sandstone	-0.60 (sh)	-0.79	-0.57	-0.82	(sh)	-0.78	-0.58	-0.80
GLO066A	caliche	-0.60	-0.79	-0.57	-0.81	(sh)	-0.76	-0.58	-0.79

C1 and C2 are the more positive and more negative cathodic peaks, respectively, (sh) denotes an unresolved peak or a shoulder, (np) indicates the absence of a voltammetric peak.

appears after heating, while in the other samples the C1 peak is enhanced after heating.

The development of the voltammetric peaks of original, extracted, heated, and extracted+heated samples was used to estimate the fractions of the ferric oxide species present in the samples as illustrated in Fig. 3. We confirmed this estimate by comparing the charges of C1 and C2 in the extracted and heated samples. GLO59A has the highest concentration of free ferric oxides and the smallest fraction of goethite (Table 5), which is in line with the estimate of ~3 wt% total Fe in the sample and the lowest $B_{1/2}$ for component 2 of all La Gloria samples. GLO62A has the smallest fraction of poorly crystalline hematite, which was confirmed by the low contribution of hard magnetic minerals in the IRM component analysis. However, this sample also has the highest concentration of goethite, which is reflected in the high $B_{1/2}$ of the hard component. In GLO65A and GLO66A the ratio of the components of the goethite–hematite assemblage is very similar, which is reflected in the magnetic characteristics as well.

4. Discussion

Magnetic analyses indicate all samples contained a mixture of magnetite and a hard component inferred to be hematite and/or goethite. VMP showed the hard component consisted of well crystalline goethite and hematite as well as poorly crystalline hematite. Magnetite could not be detected by VMP, indicating it is below the detection limit of 0.2 wt%. Assuming an SIRM for SD magnetite of 45 Am²/kg, we can calculate that the average magnetite concentration in our samples is ~0.002 wt%. This is in agreement with the VMP results.

In the samples, the magnetite is presumably of detrital origin. The crystalline hematite and goethite probably formed during deposition of the clay and sand in a warm and dry climate. Usually hematite and goethite are formed from dehydration of ferrihydrite. In warm and dry climates, the formation of hematite is favoured over that of goethite [27]. The poorly crystalline hematite could have been created during a separate soil-forming phase, hence its poor crystallinity and

Table 5

Estimates of the concentration of the three separate ferric oxide phases detected in the La Gloria samples

Sample code	Fe ₂ O ₃ (%)	Hematite (C1)	Hematite (C2)	Goethite (C2)
GLO059A	1.3 ± 0.7	0.5	0.4	0.1
GLO062A	0.4 ± 0.2	0.1	0.4	0.5
GLO065A	0.3 ± 0.2	0.4	0.3	0.3
GLO066A	0.5 ± 0.3	0.5	0.25	0.25

The second column gives the absolute percentage of iron oxides, columns 3–5 give the relative contributions of the different iron oxide phases.

small grain size. GLO62A does not contain the poorly crystalline hematite phase, but it is a sandy horizon, poor in clay, and has probably undergone little additional soil formation.

The VMP peaks are very distinct and allowed for semi-quantitative analysis of the separate contributions of these three mineral phases. The estimates of the amount of free ferric oxides obtained by voltammetry (0.1–2 wt%) were comparable to those obtained from total iron extraction (1–3 wt%) [24]. This lends further support for the internal standard technique that was used in our experiments. Since the estimated error-ranges are not that small we have assigned a semi-quantitative character to the method. The total amount of hematite in the samples varied from ~ 0.2 wt% to ~ 1.8 wt%, and could be detected by magnetic methods as well. Contrarily, the goethite was not detected by other rock-magnetic techniques, probably due to the low concentrations of ~ 0.2 to 0.6 wt% as well as the low magnetic signal of goethite compared to that of hematite. Only the magnetic signal of sample GLO62A indicated the possible presence of goethite, by an increased $B_{1/2}$ compared to the other GLO samples.

5. Conclusion

The sensitivity of voltammetry to ferric oxides is an order of magnitude better than that of XRD, and therefore we were able to detect goethite and hematite in natural samples with total free $\text{Fe}_2\text{O}_3 \geq 0.1$ –0.2 wt%. Beside the detection itself, voltammetry provided more detailed information about the ferric oxides, based on the distribution of their dissolution reactivity.

With VMP we demonstrated that AAO-Fe^{2+} extraction attacked at least part of the poorly crystalline (pedogenic) hematite in the samples. The magnetic data showed that the AAO-Fe^{2+} extraction had removed the fine-grained magnetite, and in some cases it had also dissolved part of the hard magnetic fraction (hematite) [3,25]. VMP showed that the more crystalline goethite and hematite were preserved after this treatment. The magnetic analyses are particularly suited for magnetite characterisation, but the information

on the ferric oxide phases (hematite and goethite) is substantially more detailed in the VMP data. Addition of an internal standard (pyrolusite) enables semi-quantitative evaluation of the concentration of ferric oxides.

Acknowledgements

Pauline Kruiver kindly supplied us the La Gloria samples and corresponding magnetic data. M.J.D. acknowledges CEREGE for support during his sabbatical stay. Part of this work was conducted under the programme of the Vening Meinesz Research School of Geodynamics (VMSG), and funded by the Netherlands Organisation for Scientific Research (NWO/ALW). [RV]

References

- [1] P. Fine, M.J. Singer, K.L. Verosub, J. TenPas, New evidence for the origin of ferrimagnetic minerals in loess from China, *J. Soil Sci. Soc. Am.* 57 (S5) (1993) 1537–1542.
- [2] W. Sun, S.K. Banerjee, C.P. Hunt, The role of maghemite in the enhancement of magnetic signal in the Chinese loess-paleosol sequence: An extensive rock magnetic study combined with citrate-bicarbonate-dithionite treatment, *Earth Planet. Sci. Lett.* 133 (1995) 493–505.
- [3] I.H.M. van Oorschot, M.J. Dekkers, P. Havlicek, Selective Dissolution of Magnetic Iron Oxides With the Acid-Ammonium-Oxalate/Ferrous-Iron Extraction Technique; II. Natural Loess and Palaeosol Samples, *Geophys. J. Int.*, 2002, in press.
- [4] P.W. Atkins, *General Chemistry*, Scientific American Books, New York, 1989.
- [5] F. Scholz, L. Nitschke, G. Henrion, A new procedure for fast electrochemical analysis of solid materials, *Naturwissenschaften* 76 (1989) 71–72.
- [6] P.T. Kissinger, W.R. Heineman, Laboratory techniques in Electroanalytical Chemistry, in: A.J. Bard (Ed.), *Monographs in Electroanalytical Chemistry and Electrochemistry* 5, Marcel Dekker, New York, 1984, pp. 751.
- [7] F. Scholz, B. Meyer, Voltammetry of solid microparticles immobilized on electrode surfaces, in: A.J. Bard, I. Rubinstein (Eds.), *Electroanalytical Chemistry – A series of Advances* 20, Marcel Dekker, New York, 1998, pp. 1–86.
- [8] T. Grygar, J. Subrt, J. Boháček, Electrochemical dissolution of goethite by abrasive stripping voltammetry, *Collect. Czech. Chem. Commun.* 60 (1995) 950–959.
- [9] T. Grygar, Kinetics of electrochemical reductive dissolu-

- tion of iron(III) hydroxy-oxides, *Collect. Czech. Chem. Commun.* 60 (1995) 1261–1273.
- [10] T. Grygar, Dissolution of pure and substituted goethites controlled by the surface reaction under conditions of abrasive stripping voltammetry, *J. Solid State Electrochem.* 1 (1997) 77–82.
- [11] T. Grygar, R. Kral, C. Nekovarik, P. Zelenda, *J. Czech. Geol. Soc.* 42 (1997) 121.
- [12] T. Grygar, Phenomenological kinetics of irreversible electrochemical dissolution of metal-oxide microparticles, *J. Electroanal. Chem.* 2 (1998) 127–136.
- [13] W. Krijgsman, M. Garces, C.G. Langereis, R. Daams, J. v. Dam, A.J. v.d. Meulen, J. Agusti, L. Cabrera, A new chronology for the middle to late Miocene continental record in Spain, *Earth Planet. Sci. Lett.* 142 (1996) 367–380.
- [14] A.M. Alonso-Zarza, J.P. Calvo, Palustrine sedimentation in an episodically subsiding basin: the Miocene of the northern Teruel Graben (Spain), *Palaeogeogr. Palaeoclimatol. Palaeoecol.* 160 (2000) 1–21.
- [15] P.P. Kruiver, M.J. Dekkers, D. Heslop, Quantification of magnetic coercivity components by the analysis of acquisition curves of isothermal remanent magnetisation, *Earth Planet. Sci. Lett.* 189 (2001) 269–276.
- [16] D. Heslop, M.J. Dekkers, P.P. Kruiver, I.H.M. van Oorschot, Analysis of isothermal remanent magnetisation acquisition curves using an expectation–maximisation algorithm, *Geophys. J. Int.*, in press.
- [17] C.R. Pike, A.P. Roberts, K.L. Verosub, Characterizing interactions in fine magnetic particle systems using first order reversal curves, *J. Appl. Phys.* 85 (1999) 6660–6667.
- [18] A.P. Roberts, C.R. Pike, K.L. Verosub, First-order reversal curve diagrams: A new tool for characterising the magnetic properties of natural samples, *J. Geophys. Res.* 105 (2000) 28461–28475.
- [19] C.R. Pike, A.P. Roberts, K.L. Verosub, FORC diagrams and thermal relaxation effects in magnetic particles, *Geophys. J. Int.* 145 (2001) 721–730.
- [20] F. Scholz, B. Meyer, Electrochemical solid state analysis State of the art, *Chem. Soc. Rev.* 23 (1994) 341–347.
- [21] T. Grygar, Electrochemical dissolution of iron(III) hydroxy-oxides: more information about the particles, *Collect. Czech. Chem. Commun.* 61 (1996) 93–106.
- [22] T. Grygar, The electrochemical dissolution of iron(III) and chromium(III) oxides and ferrites under conditions of abrasive stripping voltammetry, *J. Electroanal. Chem.* 405 (1996) 117–125.
- [23] T. Grygar, H.D. Ruan, Dissolution of anisotropic and anisometric prismatic particles limits of common kinetic laws, *Models Chem.* 135 (1998) 31–43.
- [24] T. Grygar, I.H.M. van Oorschot, Voltammetric identification of pedogenic iron oxides in paleosol and loess, *Electroanalysis*, in press.
- [25] I.H.M. van Oorschot, M.J. Dekkers, Selective dissolution of magnetic iron oxides in the acid-ammonium-oxalate/ferrous-iron extraction method; I; synthetic samples, *Geophys. J. Int.* 145 (2001) 740–748.
- [26] S. Bakardjieva, P. Bezdzicka, T. Grygar, P. Vorm, Reductive dissolution of microparticulate manganese oxides, *J. Solid State Electrochem.* 4 (2000) 306–313.
- [27] R.M. Cornell, U. Schwertmann, *The iron oxides*, VCH Publishers, Weinheim, 1996, 573 pp.